Supporting Information

Co-Fe Mixed Metal Phosphide Nanocubes with Highly Interconnected-Pore Architecture as an Efficient Polysulfide Mediator for Lithium-Sulfur Batteries

Yi Chen,[†] Wenxue Zhang,[‡] Dong Zhou,[†] Huajun Tian,[†] Dawei Su,[*,†] Chengyin Wang,[§] Declan Stockdale,[†] Feiyu Kang,[∥] Baohua Li,[*,∥] and Guoxiu Wang[*,†]

[†]Centre for Clean Energy Technology, School of Mathematical and Physical Sciences, Faculty of Science, University of Technology Sydney, Sydney, New South Wales 2007, Australia

[‡]School of Materials Science and Engineering, Chang'an University, Xi'an 710064, China

[§]College of Chemistry and Chemical Engineering, Yangzhou University, Yangzhou 225002, China

[∥]Graduate School at Shenzhen, Tsinghua University, Shenzhen 518055, China

[*]Corresponding authors: Dawei.Su@uts.edu.au (D. Su); libh@mail.sz.tsinghua.edu.cn (B. Li); Guoxiu.Wang@uts.edu.au (G. Wang)

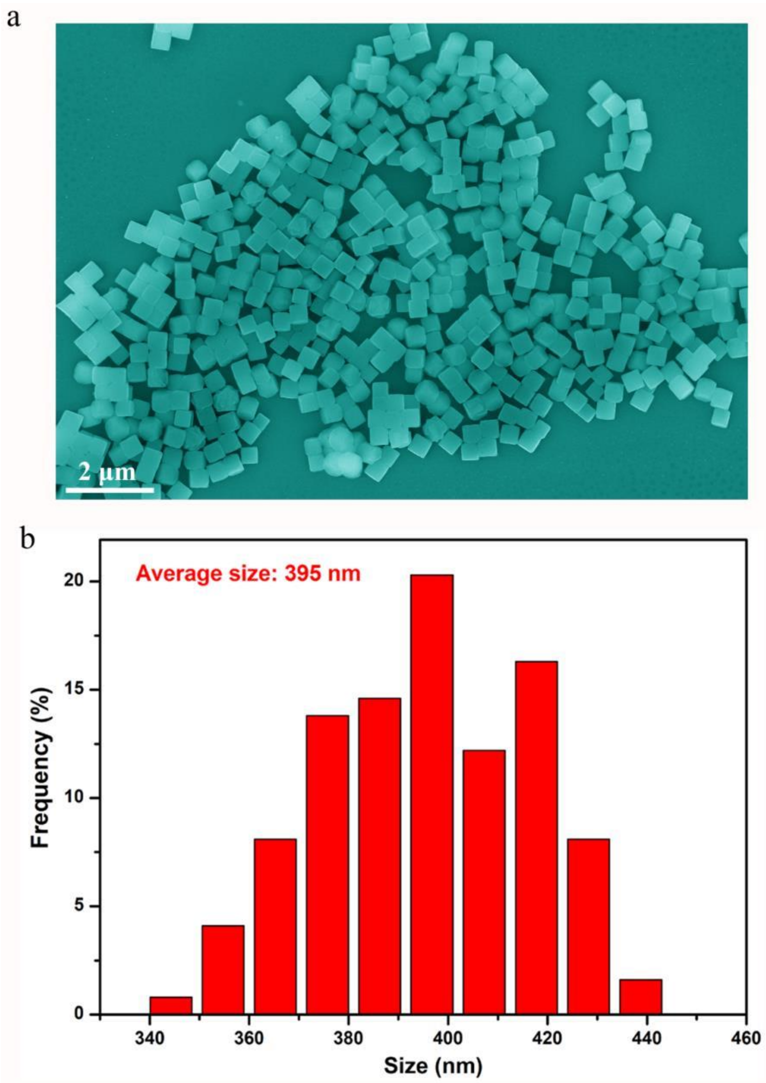

Figure S1. (a) Low resolution SEM image and (b) corresponding size distribution of $Fe_{0.667}Co(CN)_4(H_2O)_4$ nanocubes.

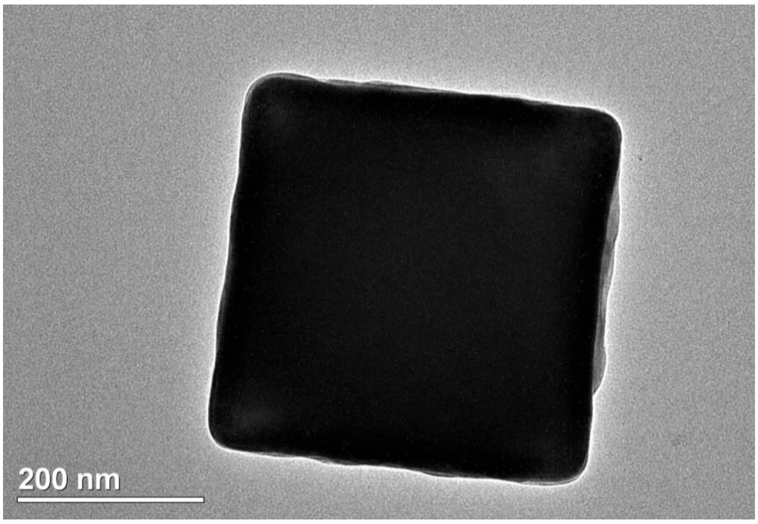

Figure S2. TEM image of a single $Fe_{0.667}Co(CN)_4(H_2O)_4$ nanocube.

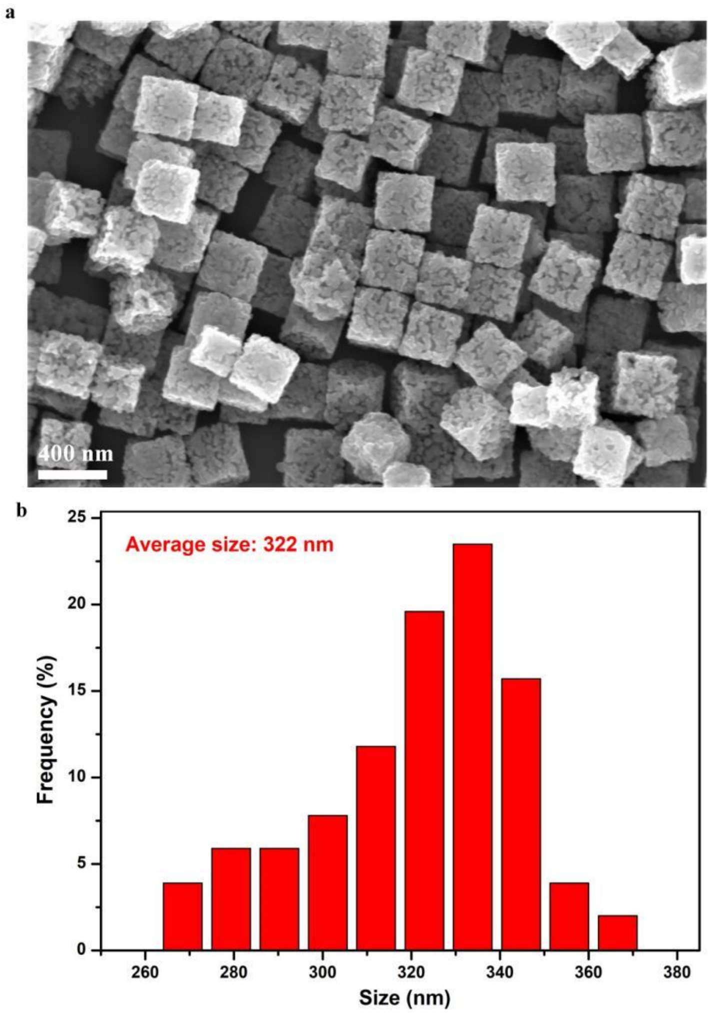

Figure S3. (a) Low resolution SEM image and (b) corresponding size distribution of Co-Fe-P nanocubes.

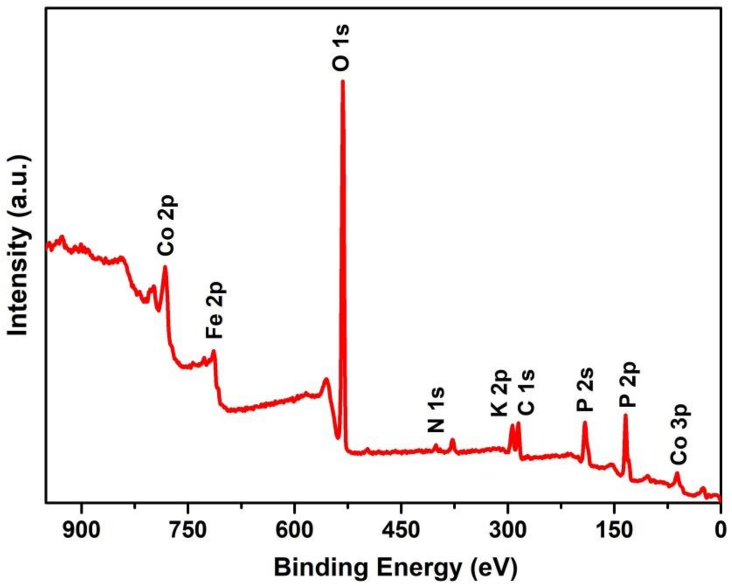

Figure S4. XPS survey spectrum of Co-Fe-P nanocubes.

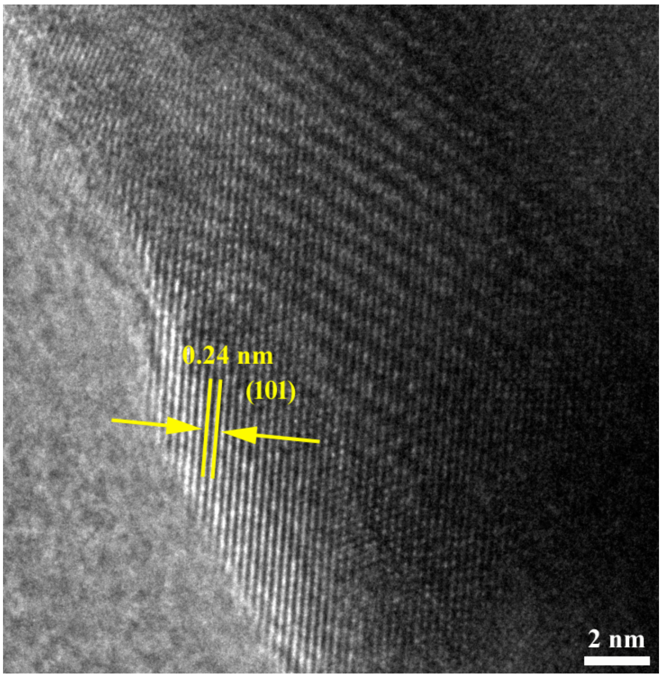

Figure S5. HR-TEM image of Co-Fe-P nanocubes. The lattice fringe is attributed to the (101) plane of FeP_2.

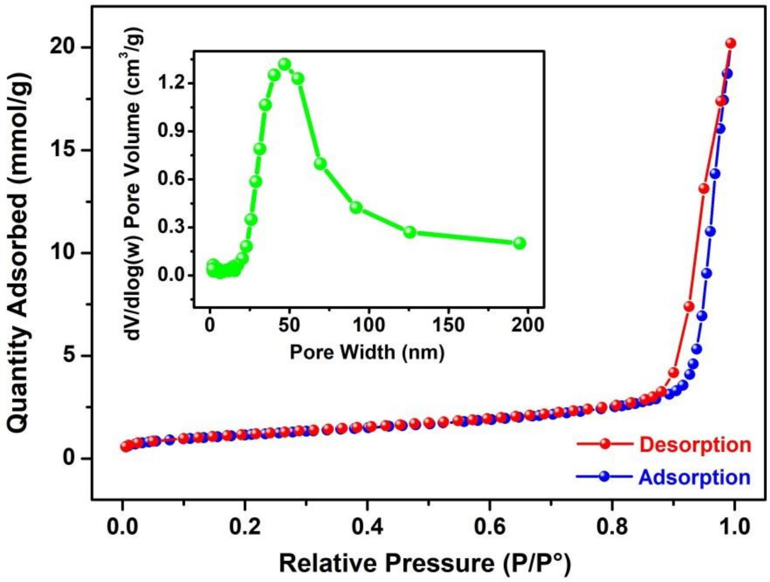

Figure S6. Nitrogen adsorption-desorption isotherm of the Co-Fe-P nanocubes. The inset shows the pore size distribution acquired using the BJH method.

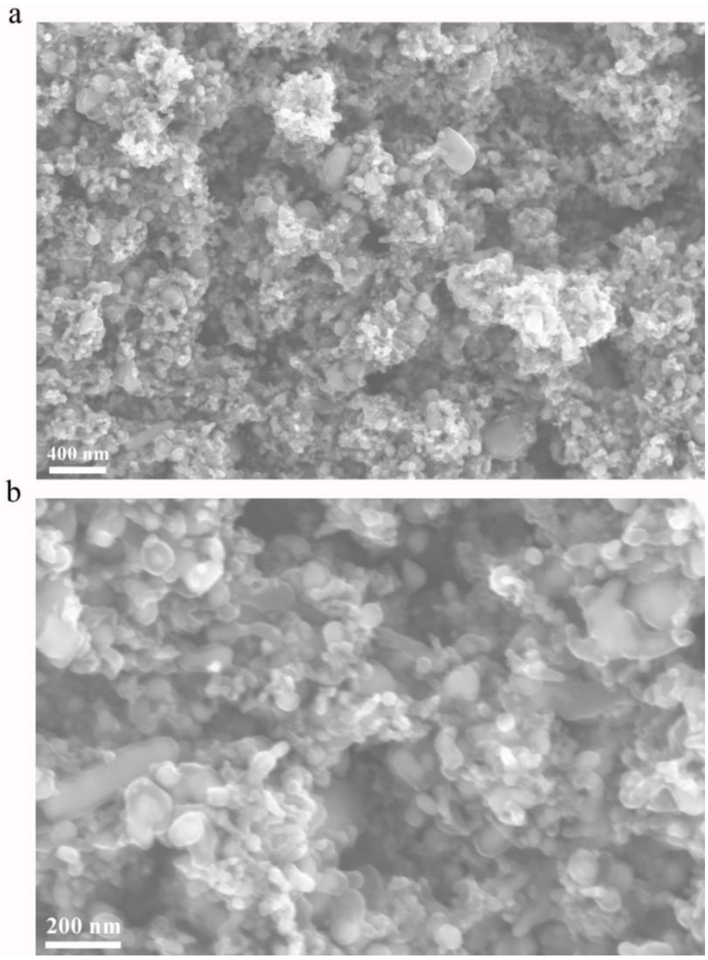

Figure S7. SEM images of Co-Fe nanoparticles.

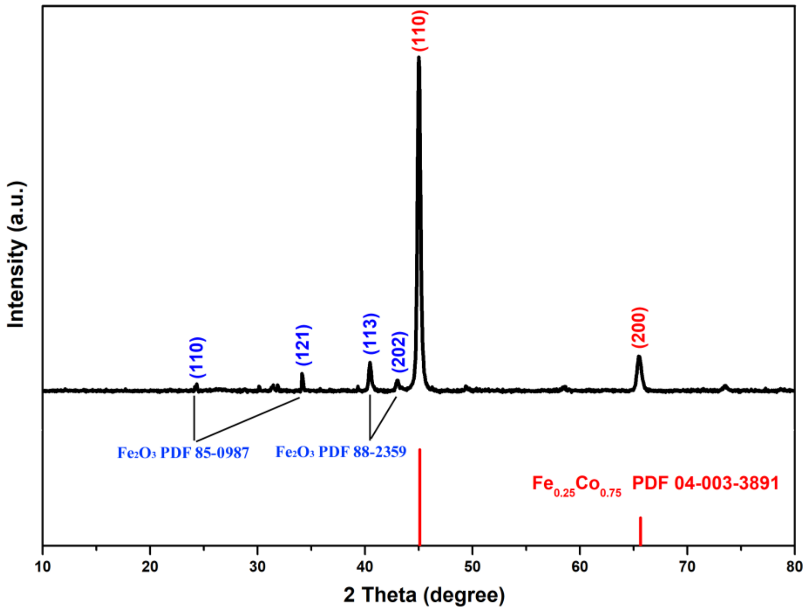

Figure S8. XRD pattern of Co-Fe nanoparticles.

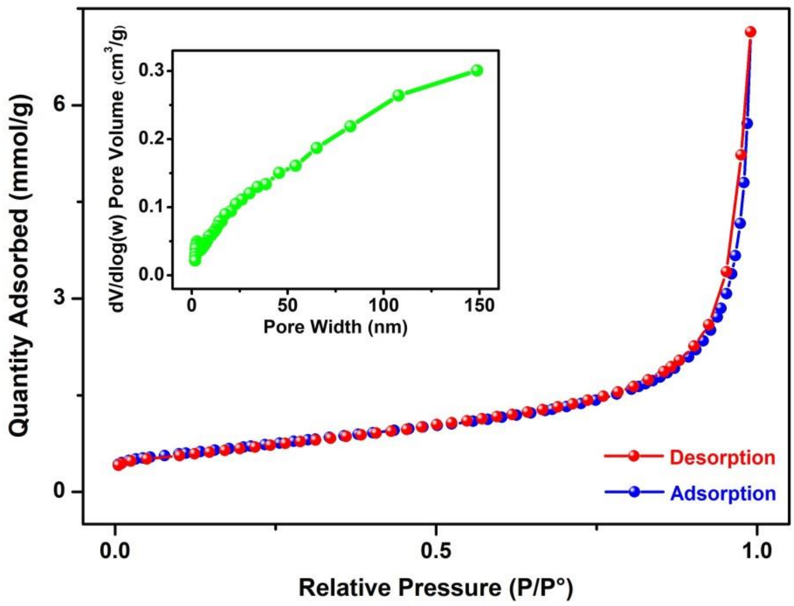

Figure S9. Nitrogen adsorption-desorption isotherm of the Co-Fe nanoparticles. The inset shows the pore size distribution obtained using the BJH method.

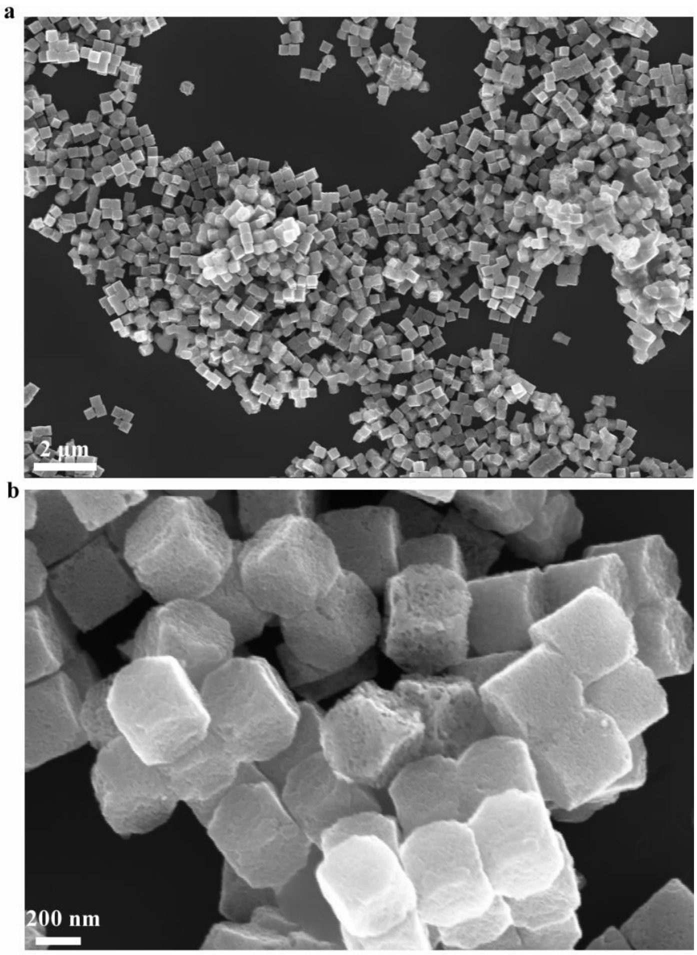

Figure S10. SEM images of Co-Fe-P nanoparticles synthesized at 500 °C.

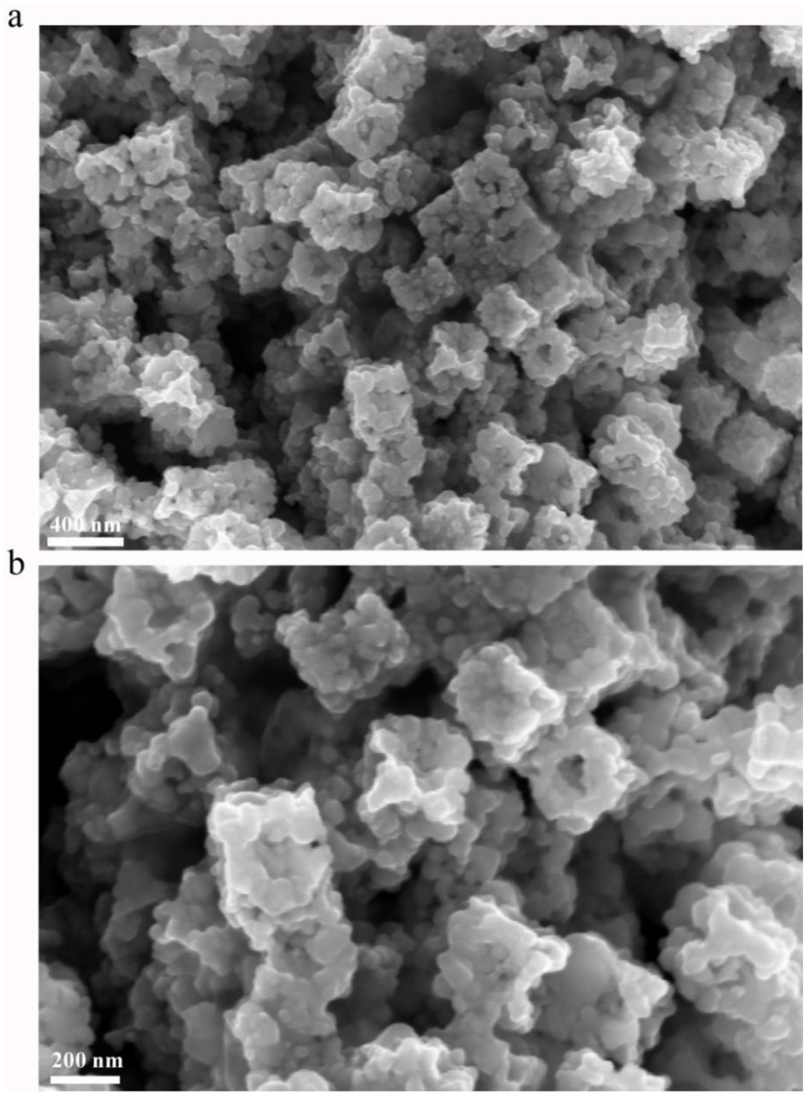

Figure S11. SEM images of Co-Fe-P nanoparticles synthesized at 650 °C.

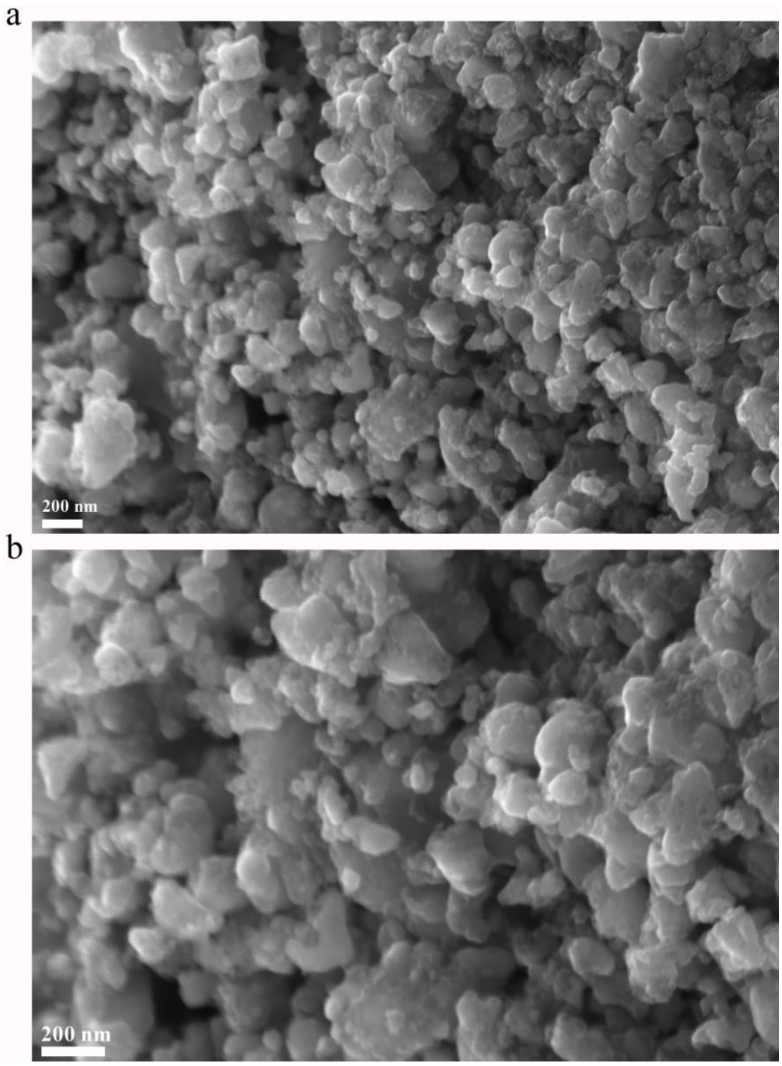

Figure S12. SEM images of Co-Fe-P nanoparticles synthesized at 700 °C.

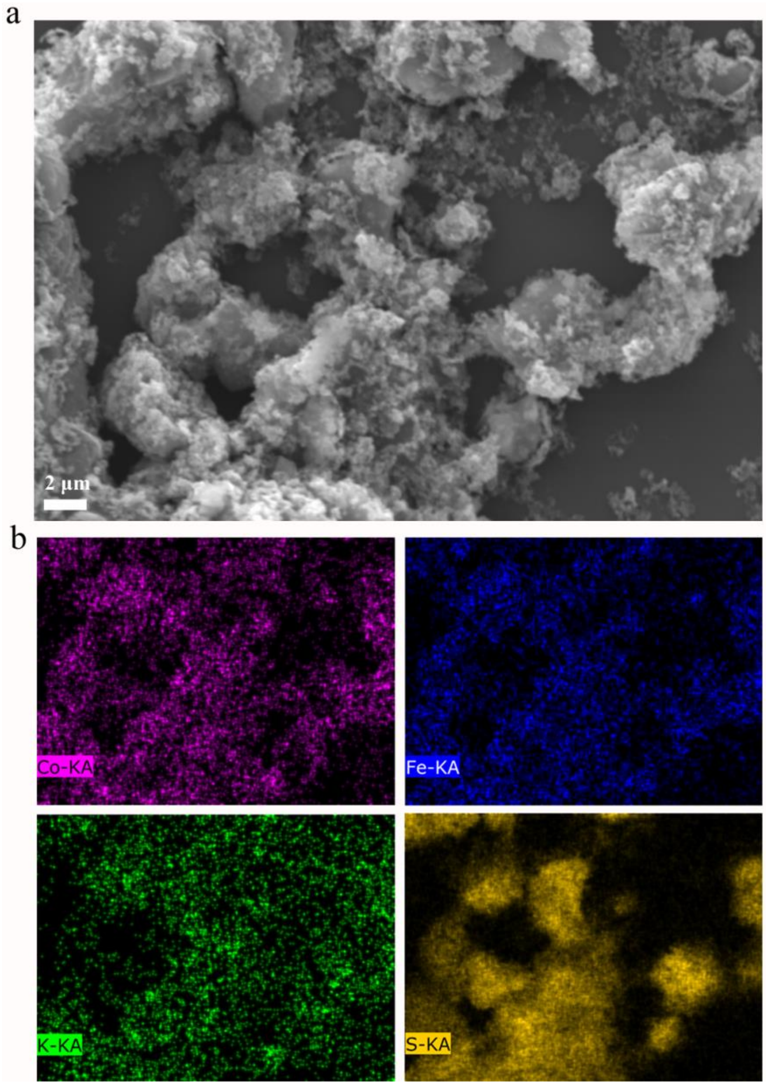

Figure S13. (a) SEM image and the (b) corresponding elemental mappings of the S@Co-Fe particles.

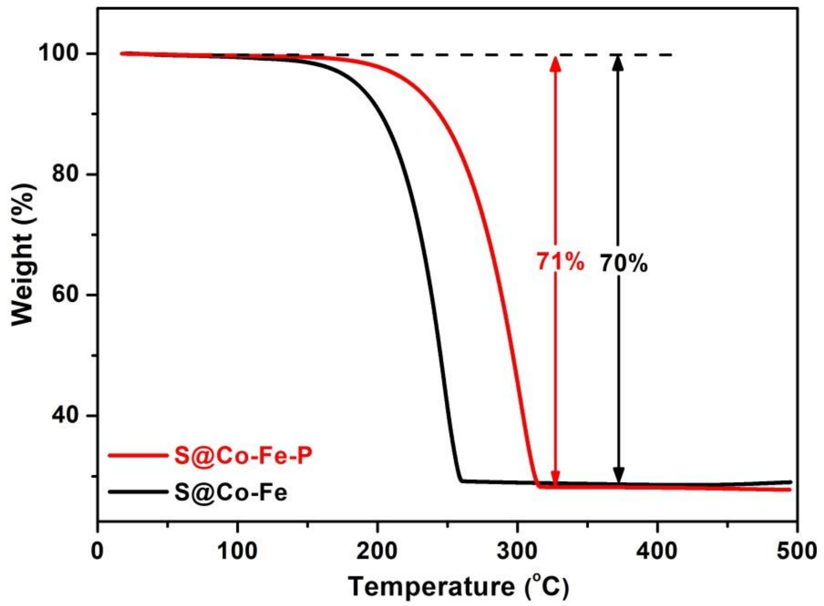

Figure S14. TGA curves of S@Co-Fe-P and S@Co-Fe nanocubes at a heating rate of 10 °C/min under Ar atmosphere.

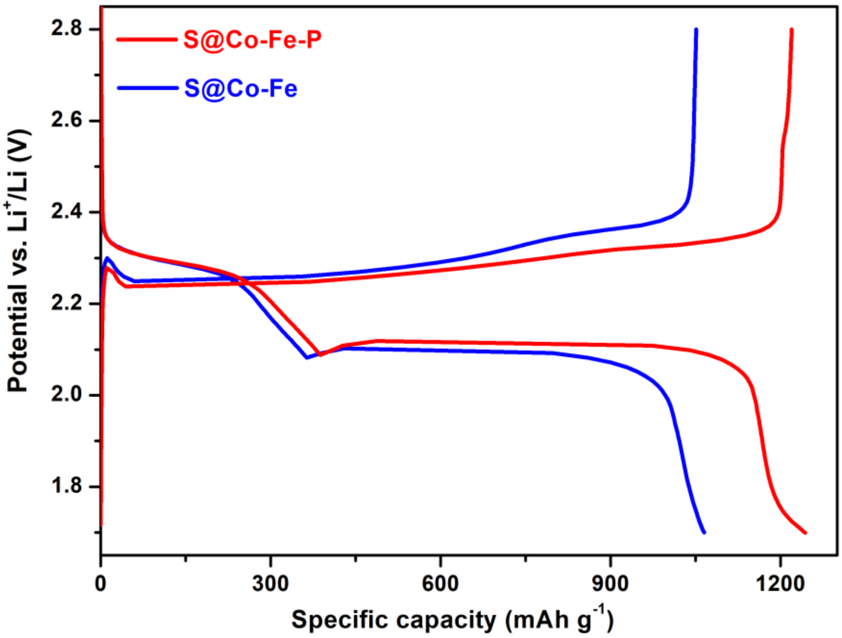

Figure S15. The galvanostatic charge-discharge voltage profiles of S@Co-Fe-P and S@Co-Fe cathodes at 0.1 C.

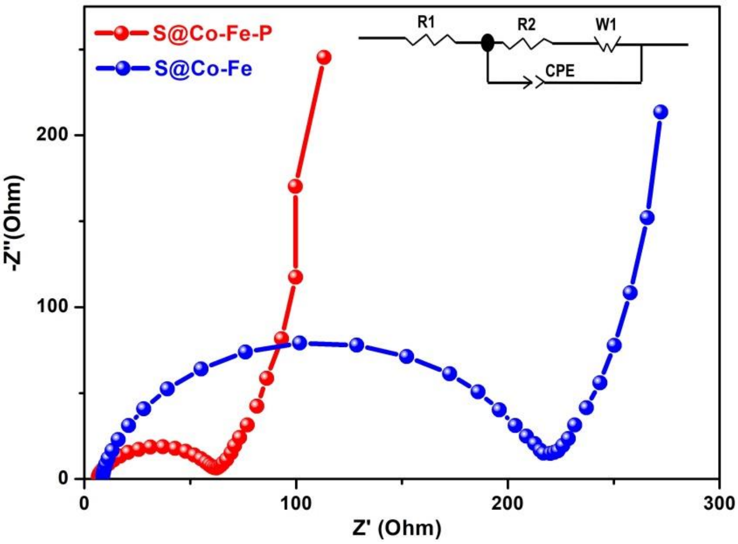

Figure S16. Nyquist plots of S@Co-Fe-P and S@Co-Fe electrodes before cycling. The inset shows equivalent circuit.

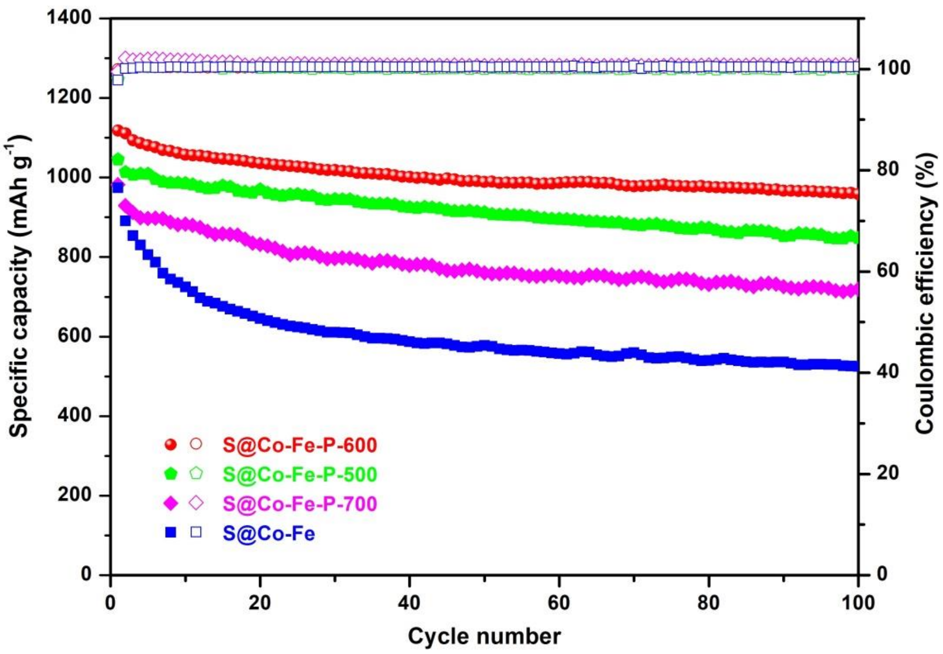

Figure S17. Cycling performances and Coulombic efficiencies of S@Co-Fe-P-600, S@Co-Fe-P-500, S@Co-Fe-P-700 and S@Co-Fe cathodes.

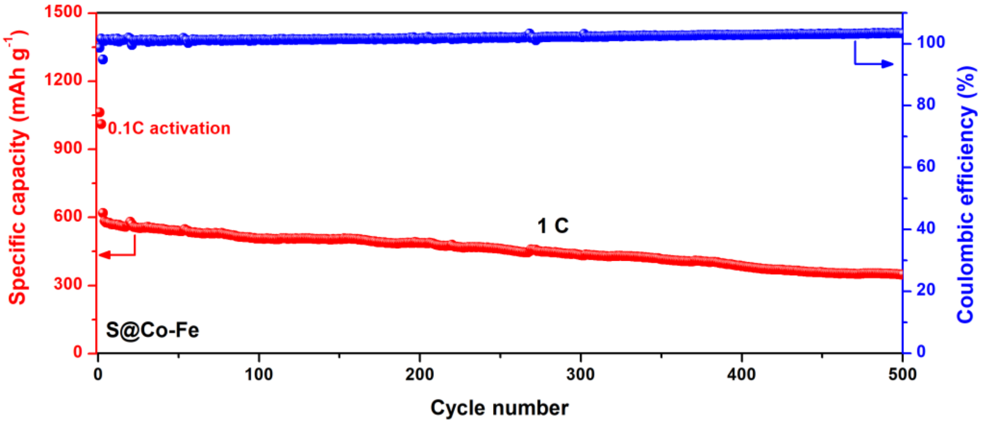

Figure S18. Cycling performance and Coulombic efficiency of the S@Co-Fe cathode at 1 C.

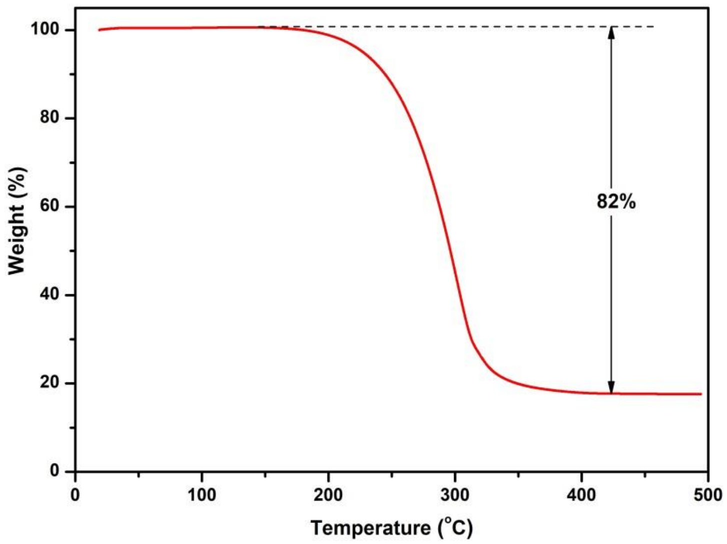

Figure S19. TGA curve of S@Co-Fe-P nanocubes with a higher sulfur content of about 82%.

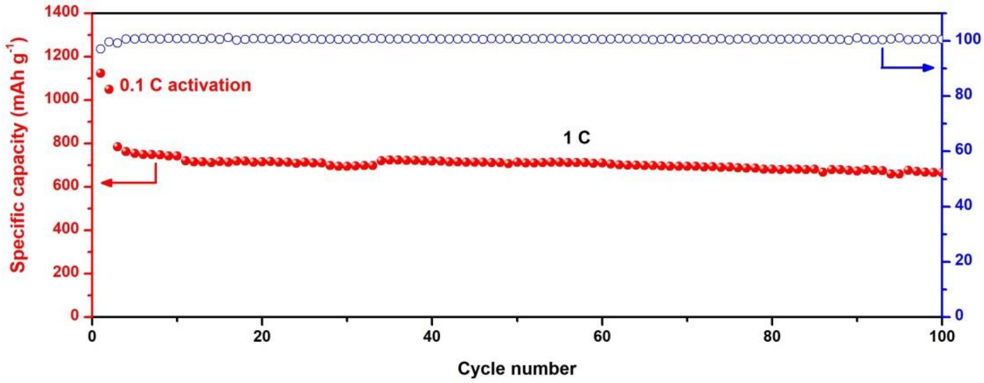

Figure S20. Cycling performance and Coulombic efficiency of S@Co-Fe-P cathode at 1C with a higher sulfur content of 82%. The areal sulfur loading is about 3 mg cm^{-2}.

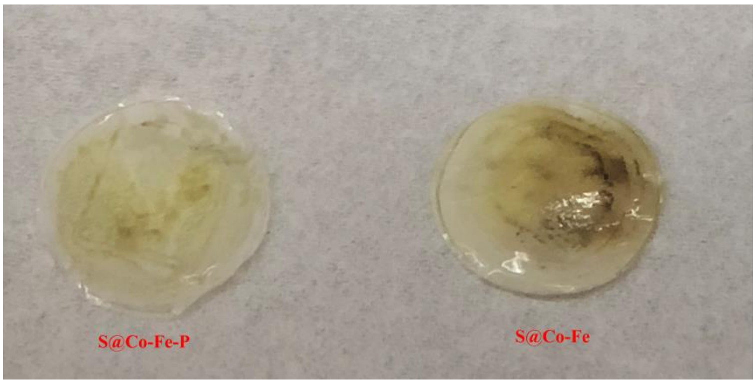

Figure S21. Digital photographs of the separators paired with S@Co-Fe-P and S@Co-Fe cathodes after 500 cycles at 1 C, respectively.

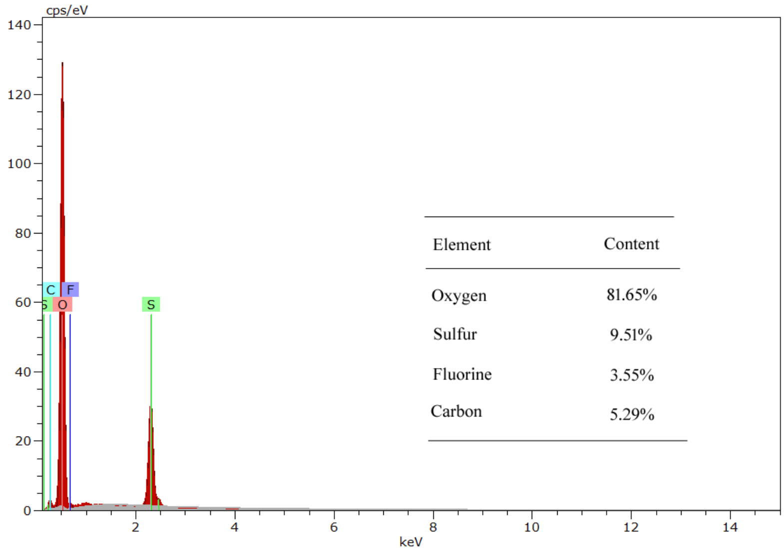

Figure S22. EDX spectrum of the lithium metal anode paired with the S@Co-Fe cathode after 500 cycles at 1 C. The inset shows the elemental contents and the carbon come from the nearby conducting substrate.

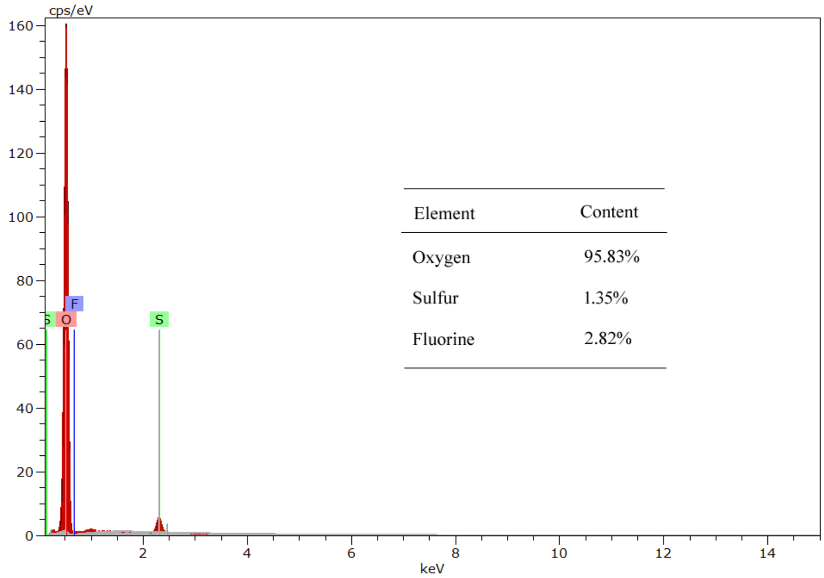

Figure S23. EDX spectrum of the lithium metal anode paired with the S@Co-Fe-P cathode after 500 cycles at 1 C. The inset shows the elemental contents.

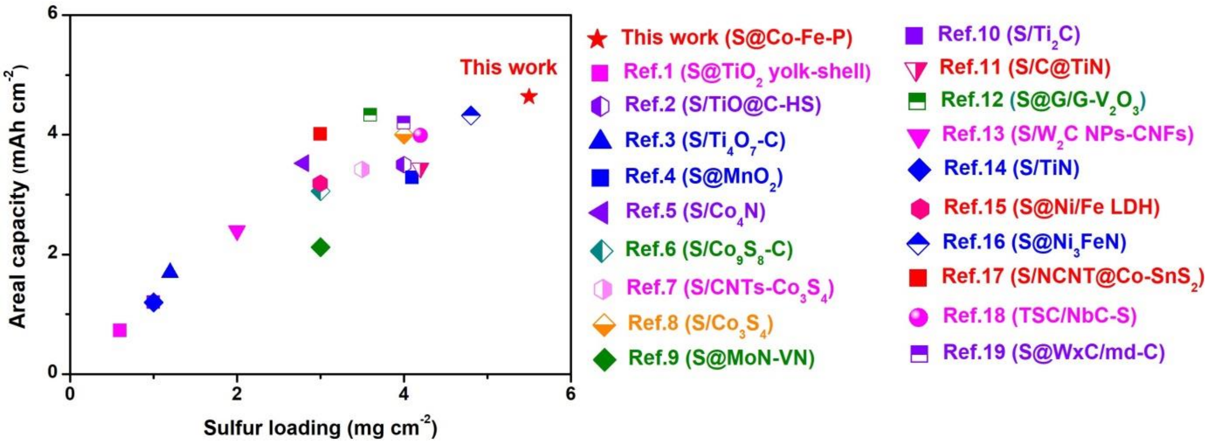

Figure S24. Comparison of the areal capacity of this work with other reported metal compounds as sulfur host materials for Li-S batteries. [1-19]

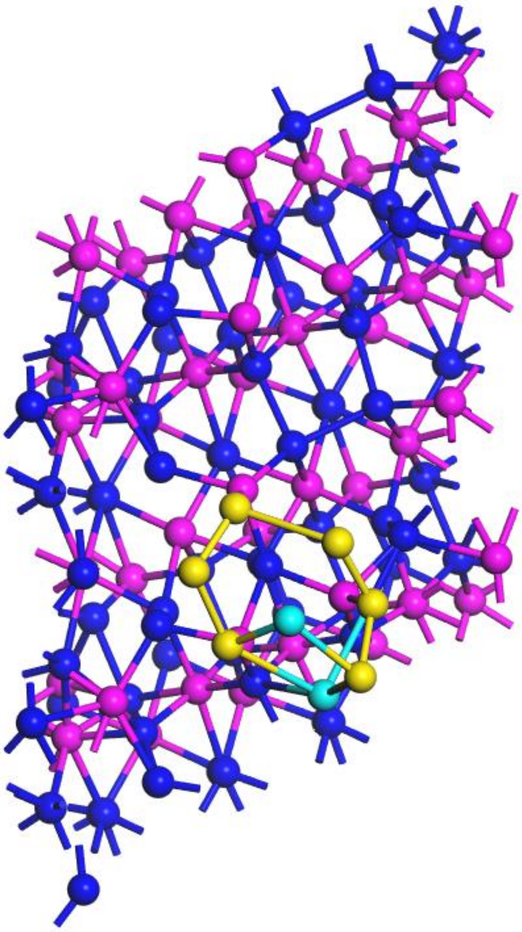

Figure S25. Top view of a Li_2S_6 molecule adsorbed on the (-111) plane of CoP_2 using DFT calculations. The pink, blue, yellow and light blue balls represent Co, P, S and Li atoms, respectively.

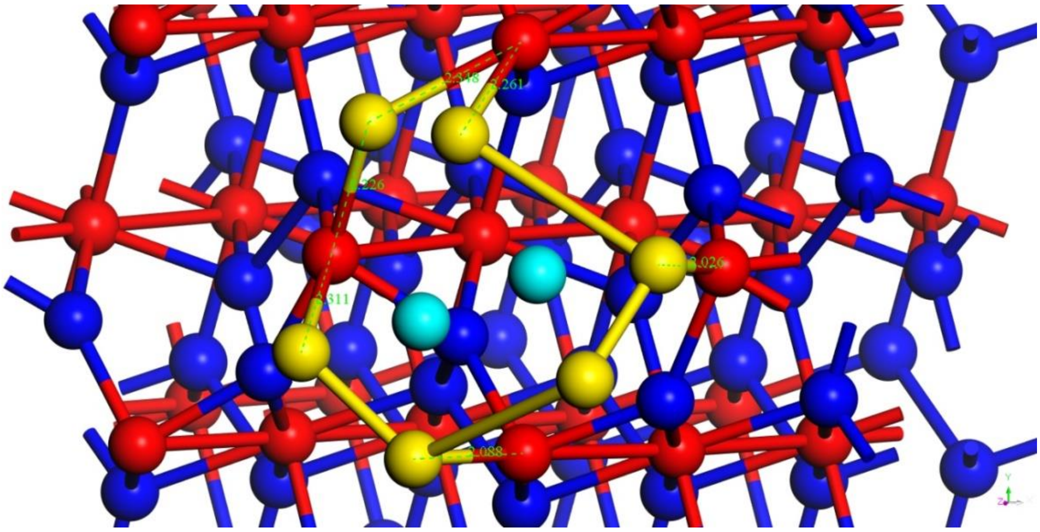

Figure S26. Top view of a Li_2S_6 molecule adsorbed on the (101) plane of FeP_2 using DFT calculations. The red, blue, yellow and light blue balls represent Fe, P, S and Li atoms, respectively.

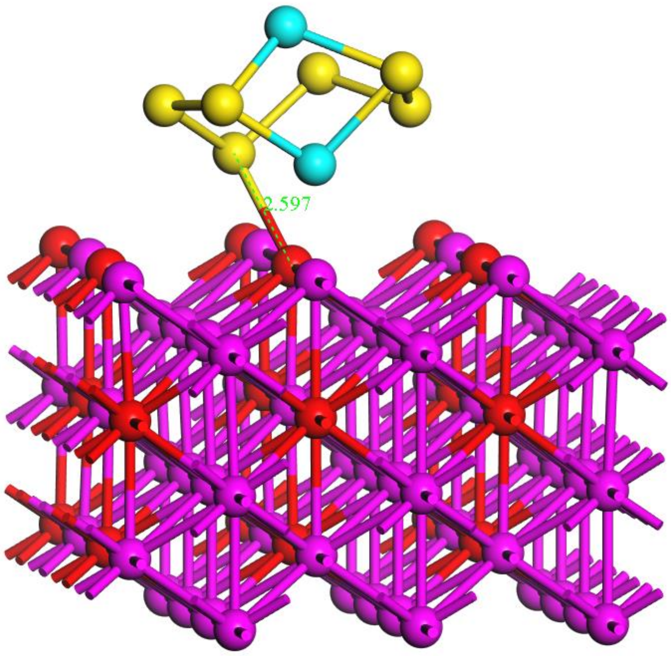

Figure S27. Side view a Li_2S_6 molecule adsorbed on the (110) plane of $Fe_{0.25}Co_{0.75}$ using DFT calculations. The binding energy is calculated to be -1.11 eV. The pink, red, yellow and light blue balls represent Co, Fe, S and Li atoms, respectively.

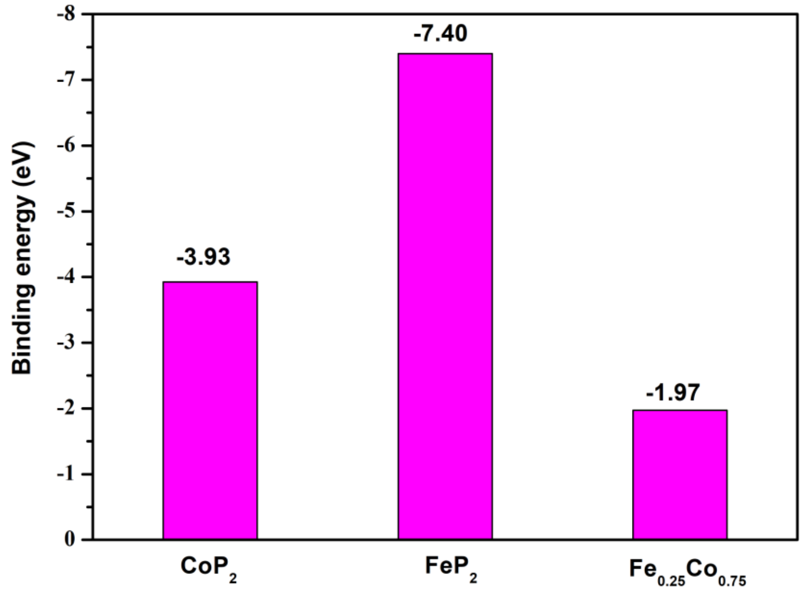

Figure S28. The calculated binding energies between Li_2S_6 and CoP_2, FeP_2 and $Fe_{0.25}Co_{0.75}$ (111).

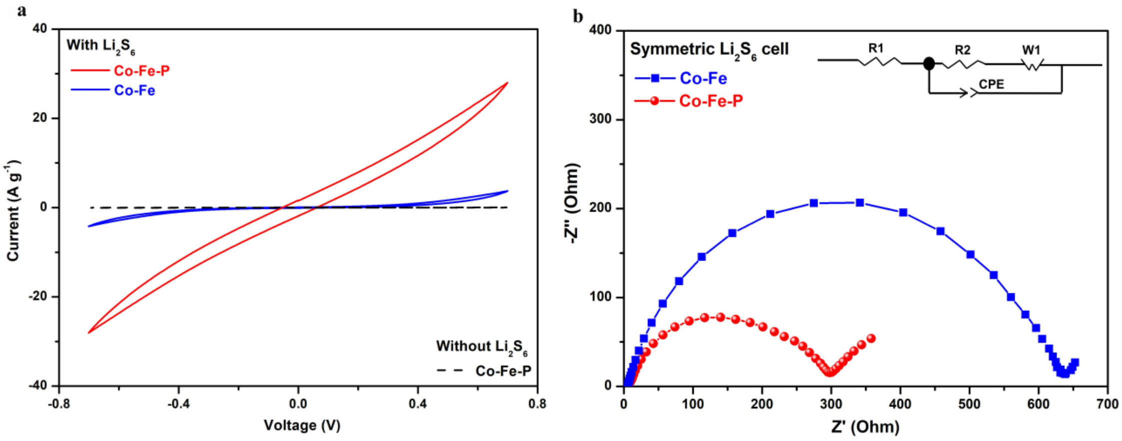

Figure S29. (a) CV curves of Li_2S_6 and Li_2S_6-free symmetric cells. (b) EIS spectra of symmetric Li_2S_6 cells. The inset in Figure b shows equivalent circuit.

Table S1. Parameters identified by modeling the impedance spectra in **Figure S16**.

Working Electrode	R_e (Ω)	R_{ct} (Ω)	Y1($\Omega^{-1}cm^{-2}s^{-n}$)	n1
S@Co-Fe-P	5.761	56.81	2.46×10^{-5}	0.74
S@Co-Fe	8.003	205.8	4.89×10^{-6}	0.85

Table S2. Parameters identified by modeling the impedance spectra of Li_2S_6 symmetric cells in **Figure S29**.

Working Electrode	R_e (Ω)	R_{ct} (Ω)	Y1($\Omega^{-1}cm^{-2}s^{-n}$)	n1
Co-Fe-P	4.352	352	3.86×10^{-5}	0.70
Co-Fe	5.356	613.3	1.89×10^{-5}	0.79

Table S3. Comparison of the cycling performance of this work with other previously reported metal compounds as sulfur host materials for Li-S batteries.

Name	Initial capacity (mAh g^{-1})	Cycle number	Current rate (C)	Capacity decay rate per cycle (%)
This work	**863**	**500**	**1**	**0.043**
S/WO_3[20]	769	100	0.2	0.56
C@TiO_2@C–S[21]	774	500	2	0.068
Ni_3S_2[22]	526	300	0.5	0.24
S/Ti_4O_7[23]	850	500	2	0.059
NbS_2@S@IG[24]	500	600	1	0.033
S/TiS_2[22]	700	300	0.5	0.073
S/TiO-Graphene[25]	831	200	2	0.226
a-Ti_3C_2−S/d-Ti_3C_2/PP[26]	800	200	2	0.248
S/FeS[22]	705	300	0.5	0.175
S/W_2C NPs-CNFs[13]	864	500	1	0.06
S/SnS_2[22]	610	300	0.5	0.229
S/TiN[14]	988	500	0.5	0.07
S/ VS_2[22]	830	300	0.5	0.052
S/WC[20]	843	100	0.2	0.18
S/MgO[27]	860	100	0.2	0.18
S/CoS_2[22]	684	300	0.5	0.05

REFERENCES

(1) Seh, Z. W.; Li, W.; Cha, J. J.; Zheng, G.; Yang, Y.; McDowell, M. T.; Hsu, P.-C.; Cui, Y., Sulphur-TiO_2 Yolk-Shell Nanoarchitecture with Internal Void Space for Long-Cycle Lithium-Sulphur Batteries. *Nat. Commun.* **2013**, *4*, 1331.
(2) Li, Z.; Zhang, J.; Guan, B.; Wang, D.; Liu, L.-M.; Lou, X. W. D., A Sulfur Host Based on Titanium Monoxide@Carbon Hollow Spheres for Advanced Lithium-Sulfur Batteries. *Nat. Commun.* **2016**, *7*, 13065.
(3) Mei, S.; Jafta, C. J.; Lauermann, I.; Ran, Q.; Kärgell, M.; Ballauff, M.; Lu, Y., Porous Ti_4O_7 Particles with Interconnected-Pore Structure as a High-Efficiency Polysulfide Mediator for Lithium-Sulfur Batteries. *Adv. Funct. Mater.* **2017**, *27*, 1701176.
(4) Liang, X.; Nazar, L. F., In Situ Reactive Assembly of Scalable Core–Shell Sulfur-MnO_2 Composite Cathodes. *ACS Nano* **2016**, *10*, 4192-4198.
(5) Deng, D.-R.; Xue, F.; Jia, Y.-J.; Ye, J.-C.; Bai, C.-D.; Zheng, M.-S.; Dong, Q.-F., Co_4N Nanosheet Assembled Mesoporous Sphere as a Matrix for Ultrahigh Sulfur Content Lithium–Sulfur Batteries. *ACS Nano* **2017**, *11*, 6031-6039.
(6) Chen, T.; Ma, L.; Cheng, B.; Chen, R.; Hu, Y.; Zhu, G.; Wang, Y.; Liang, J.; Tie, Z.; Liu, J., Metallic and Polar Co_9S_8 Inlaid Carbon Hollow Nanopolyhedra as Efficient Polysulfide Mediator for Lithium-Sulfur Batteries. *Nano Energy* **2017**, *38*, 239-248.
(7) Chen, T.; Zhang, Z.; Cheng, B.; Chen, R.; Hu, Y.; Ma, L.; Zhu, G.; Liu, J.; Jin, Z., Self-Templated Formation of Interlaced Carbon Nanotubes Threaded Hollow Co_3S_4 Nanoboxes for High-Rate and Heat-Resistant Lithium-Sulfur Batteries. *J. Am. Chem. Soc.* **2017**, *139*, 12710-12715.
(8) Pu, J.; Shen, Z.; Zheng, J.; Wu, W.; Zhu, C.; Zhou, Q.; Zhang, H.; Pan, F., Multifunctional Co_3S_4@Sulfur Nanotubes for Enhanced Lithium-Sulfur Battery Performance. *Nano Energy* **2017**, *37*, 7-14.
(9) Ye, C.; Jiao, Y.; Jin, H.; Slattery, A. D.; Davey, K.; Wang, H.; Qiao, S. Z., 2D MoN-VN Heterostructure To Regulate Polysulfides for Highly Efficient Lithium-Sulfur Batteries. *Angew. Chem. Int. Ed.* **2018**, *57*, 16703-16707.
(10) Liang, X.; Garsuch, A.; Nazar, L. F., Sulfur Cathodes Based on Conductive MXene Nanosheets for High-Performance Lithium-Sulfur Batteries. *Angew. Chem. Int. Ed.* **2015**, *54*, 3907-3911.
(11) Wang, Y.; Zhang, R.; Pang, Y.-C.; Chen, X.; Lang, J.; Xu, J.; Xiao, C.; Li, H.; Xi, K.; Ding, S., Carbon@Titanium Nitride Dual Shell Nanospheres as Multi-Functional Hosts for Lithium Sulfur Batteries. *Energy Storage Mater.* **2019**, *16*, 228-235.
(12) Song, Y.; Zhao, W.; Wei, N.; Zhang, L.; Ding, F.; Liu, Z.; Sun, J., In-Situ PECVD-Enabled Graphene-V_2O_3 Hybrid Host for Lithium-Sulfur Batteries. *Nano Energy* **2018**, *53*, 432-439.
(13) Zhou, F.; Li, Z.; Luo, X.; Wu, T.; Jiang, B.; Lu, L.-L.; Yao, H.-B.; Antonietti, M.; Yu, S.-H., Low Cost Metal Carbide Nanocrystals as Binding and Electrocatalytic Sites for High Performance Li-S Batteries. *Nano Lett.* **2018**, *18*, 1035-1043.
(14) Cui, Z.; Zu, C.; Zhou, W.; Manthiram, A.; Goodenough, J. B., Mesoporous Titanium Nitride-Enabled Highly Stable Lithium-Sulfur Batteries. *Adv. Mater.* **2016**, *28*, 6926-6931.

(15) Zhang, J.; Li, Z.; Chen, Y.; Gao, S.; Lou, X. W., Nickel-Iron Layered Double Hydroxide Hollow Polyhedrons as a Superior Sulfur Host for Lithium-Sulfur Batteries. *Angew. Chem. Int. Ed.* **2018**, *57*, 10944-10948.
(16) Zhao, M.; Peng, H. J.; Zhang, Z. W.; Li, B. Q.; Chen, X.; Xie, J.; Chen, X.; Wei, J. Y.; Zhang, Q.; Huang, J. Q., Activating Inert Metallic Compounds for High-Rate Lithium-Sulfur Batteries Through In Situ Etching of Extrinsic Metal. *Angew. Chem. Int. Ed.* **2019**, *58*, 3779-3783.
(17) Gao, X.; Yang, X.; Li, M.; Sun, Q.; Liang, J.; Luo, J.; Wang, J.; Li, W.; Liang, J.; Liu, Y., Cobalt-Doped SnS_2 with Dual Active Centers of Synergistic Absorption-Catalysis Effect for High-S Loading Li-S Batteries. *Adv. Funct. Mater.* **2019**, 29, 1806724.
(18) Shen, S.; Xia, X.; Zhong, Y.; Deng, S.; Xie, D.; Liu, B.; Zhang, Y.; Pan, G.; Wang, X.; Tu, J., Implanting Niobium Carbide into Trichoderma Spore Carbon: a New Advanced Host for Sulfur Cathodes. *Adv. Mater.* **2019**, 1900009.
(19) Wu, Y.; Zhu, X.; Li, P.; Zhang, T.; Li, M.; Deng, J.; Huang, Y.; Ding, P.; Wang, S.; Zhang, R., Ultradispersed WxC Nanoparticles Enable Fast Polysulfide Interconversion for High-Performance Li-S Batteries. *Nano Energy* **2019**, *59*, 636-643.
(20) Choi, J.; Jeong, T.-G.; Cho, B. W.; Jung, Y.; Oh, S. H.; Kim, Y.-T., Tungsten Carbide as a Highly Efficient Catalyst for Polysulfide Fragmentations in Li-S Batteries. *J. Phys. Chem. C* **2018**, *122*, 7664-7669.
(21) Fang, M.; Chen, Z.; Liu, Y.; Quan, J.; Yang, C.; Zhu, L.; Xu, Q.; Xu, Q., Design and Synthesis of Novel Sandwich-Type C@TiO_2@C Hollow Microspheres as Efficient Sulfur Hosts for Advanced Lithium-Sulfur Batteries. *J. Mater. Chem. A* **2018**, *6*, 1630-1638.
(22) Zhou, G.; Tian, H.; Jin, Y.; Tao, X.; Liu, B.; Zhang, R.; Seh, Z. W.; Zhuo, D.; Liu, Y.; Sun, J., Catalytic Oxidation of Li_2S on the Surface of Metal Sulfides for Li-S Batteries. *Proc. Natl. Acad. Sci. U S A* **2017**, *114*, 840-845.
(23) Pang, Q.; Kundu, D.; Cuisinier, M.; Nazar, L., Surface-Enhanced Redox Chemistry of Polysulphides on a Metallic and Polar Host for Lithium-Sulphur Batteries. *Nat. Commun.* **2014**, *5*, 4759.
(24) Xiao, Z.; Yang, Z.; Zhang, L.; Pan, H.; Wang, R., Sandwich-Type NbS_2@S@I-Doped Graphene for High-Sulfur-Loaded, Ultrahigh-Rate, and Long-Life Lithium-Sulfur Batteries. *ACS Nano* **2017**, *11*, 8488-8498.
(25) Chen, Y.; Choi, S.; Su, D.; Gao, X.; Wang, G., Self-Standing Sulfur Cathodes Enabled by 3D Hierarchically Porous Titanium Monoxide-Graphene Composite Film for High-Performance Lithium-Sulfur Batteries. *Nano Energy* **2018**, *47*, 331-339.
(26) Dong, Y.; Zheng, S.; Qin, J.; Zhao, X.; Shi, H.; Wang, X.; Chen, J.; Wu, Z.-S., All-MXene-Based Integrated Electrode Constructed by Ti_3C_2 Nanoribbon Framework Host and Nanosheet Interlayer for High-Energy-Density Li-S Batteries. *ACS Nano* **2018**, *12*, 2381-2388.
(27) Ponraj, R.; Kannan, A. G.; Ahn, J. H.; Kim, D.-W., Improvement of Cycling Performance of Lithium-Sulfur Batteries by Using Magnesium Oxide as a Functional Additive for Trapping Lithium Polysulfide. *ACS Appl. Mater. Interfaces* **2016**, *8*, 4000-4006.